Received: 25 January 2023 | Revised: 10 June 2023 | Accepted: 7 July 2023

DOI: 10.1002/qj.4539

Quarterly Journal of the Royal Meteorological Society RMetS

RESEARCH ARTICLE

The contribution of a mesoscale cyclone and associated meteotsunami to the exceptional flood in Venice on November 12, 2019

Christian Ferrarin[1] | **Mirko Orlić**[2] | **Marco Bajo**[1] | **Silvio Davolio**[3] | **Georg Umgiesser**[1] | **Piero Lionello**[4]

[1]CNR – National Research Council of Italy, ISMAR – Institute of Marine Sciences, Venice, Italy

[2]Department of Geophysics, Faculty of Science, University of Zagreb, Zagreb, Croatia

[3]CNR – National Research Council of Italy, ISAC – Institute of Atmospheric Sciences and Climate, Bologna, Italy

[4]Department of Biological and Environmental Sciences and Technologies, University of Salento, Lecce, Italy

Correspondence
Christian Ferrarin, CNR–National Research Council of Italy, ISMAR–Marine Sciences Institute, Venice, Italy.
Email: c.ferrarin@ismar.cnr.it

Funding information
European Cooperation in Science and Technology, Grant/Award Number: MedCyclones-CA19109; Hrvatska Zaklada za Znanost, Grant/Award Number: MAUD-IP-2018-01-9849; EU Interreg Italy-Croatia, Grant/Award Number: STREAM-10249186

Abstract

On November 12, 2019, an exceptional flood event took place in Venice, second only to the one that occurred on November 4, 1966. The sea level reached a peak value of 1.89 m above the local datum determining the flooding of almost 90% of the pedestrian surface of the historical city. Several processes concurred to raise the water level in Venice and the northern Adriatic Sea on November 12, 2019. Among these, a fast-moving mesoscale cyclone travelled at about 12 m · s^{-1} in the northwestward direction over the northern Adriatic Sea, raising the sea levels at the shore in front of the Lagoon of Venice. High-resolution numerical simulations indicated that atmosphere–ocean resonance occurred on November 12, 2019, generating a meteotsunami-like wave that contributed significantly to the extreme sea level in Venice. The relative contributions of the wind and air pressure to the peak sea level were also estimated. Additional numerical experiments were performed to prove the occurrence of Proudman resonance and to determine a transfer function of such high-frequency sea-level perturbations for the Lagoon of Venice.

KEYWORDS

mesoscale cyclone, atmosphere–ocean resonance, meteotsunami, coastal flooding, Venice

1 | INTRODUCTION

One of the biggest hazards to Mediterranean coastal communities is the occurrence of destructive sea storms produced by intense cyclones that cause floods, beach erosion, damage to infrastructure, and loss of cultural heritage (Lionello *et al.*, 2019; Patlakas *et al.*, 2021; Flaounas *et al.*, 2022). The shallow northern Adriatic Sea is the Mediterranean sub-basin where storm surges reach their highest values (Marcos *et al.*, 2009), triggered mainly by a strong southeasterly moist and warm wind, called Sirocco, generally caused by cyclones generated in the western Mediterranean Sea (Lionello *et al.*, 2012; Cavaleri *et al.*, 2019; Lionello *et al.*, 2021). Indeed, the most extreme storm surge and high wave events (in 1966, 1979, and 2018) were driven by such a synoptic situation (Lionello

et al., 2021, and references therein). However, severe sea storms are not limited to the Adriatic Sea and several other segments of the Mediterranean coast are strongly impacted by cyclones. As an example, a low-pressure system, named *Gloria*, determined in 2020 the most extreme wave and storm surge ever recorded along the eastern Iberian Peninsula and caused floods, damage to coastal infrastructures, coastal erosion, and a total of 13 fatalities (Amores *et al.*, 2020). Moreover, in the Mediterranean Sea, intense cyclones showing tropical-like features (known in the scientific literature as medicanes, an abbreviation of Mediterranean hurricanes; Miglietta, 2019) sometimes develop and hit the coast severely (Patlakas *et al.*, 2021; Scicchitano *et al.*, 2021; Toomey *et al.*, 2022).

Apart from storm surges and high waves induced by cyclones, the Mediterranean Sea is also impacted by meteotsunami, destructive tsunami-like waves of an atmospheric origin (Monserrat *et al.*, 2006). When the perturbation's propagation speed approaches that of shallow-water barotropic waves, resonance in the open sea produces such high-frequency sea-level oscillations. Coastal resonance also contributes significantly to the local amplification of meteotsunami waves in harbours and bays. Several coastal regions around the Mediterranean coast, particularly those along the eastern Adriatic coast and the Balearic Islands, experienced floods and breakages as a result of a meteotsunami (Vilibić and Šepić, 2009; Orlić, 2015; Vilibić *et al.*, 2021).

Both storm surges, induced by Sirocco winds over the Adriatic associated with a deep low-pressure system over the Tyrrhenian Sea, and a meteotsunami, generated by a fast-moving mesoscale cyclone travelling northwestward along the Italian coast of the Adriatic Sea, contributed to the exceptional flood that took place in Venice on November 12, 2019 (Cavaleri *et al.*, 2020; Ferrarin *et al.*, 2021; Miglietta et al., 2023). The sea level in Venice reached the extreme value of 1.89 m (above the local datum), causing the flooding of about 90% of the city centre.

Even if such an event has been investigated deeply through the analysis of observations and the use of numerical models, the generation of the meteotsunami and how it contributed to the exceptional flood in Venice have not yet been examined in detail. Therefore, the present research aims to use numerical models for (i) investigating the relative roles of wind and air pressure forcing associated with the fast-moving local depression during the November 12, 2019 event (Section 3.2), (ii) exploring to what extent the resonance contributed to the amplification of waves along the coast (Section 3.3), (iii) checking whether the mesoscale atmospheric perturbation was coupled to gravity waves (Proudman resonance; Proudman, 1929) or edge waves (Greenspan resonance; Greenspan, 1956) in the coastal sea (Section 3.4), and (iv) determining the propagation of high-frequency sea-level perturbations from the open sea into the Lagoon of Venice (Section 3.5).

2 | METHODS

2.1 | Observational dataset

Several tide gauge and meteorological monitoring stations are operational in the northern Adriatic Sea (Ferrarin *et al.*, 2020). Among the different observational sites, we considered one meteorological station in the shelf sea (the Acqua Alta oceanographic tower located 15 km offshore: AAOT) and near the mouth of the Po River (FPO), and the tide gauges of AAOT, Diga Sud Chioggia (DSC), and Venice Punta della Salute (PDS) (Figures 1b), where, according to Ferrarin *et al.* (2021), the sea level was influenced by the mesoscale cyclone on November 12, 2019. All the sea-level values described in this study are referred to the historic Punta della Salute local datum (called ZMPS; established on the basis of 25 years of tidal surveys, from 1885–1909).

Tide-gauge data were analysed with the UTIDE Python tidal harmonic analysis tool (Codiga, 2011) to distinguish between the tidal and residual (mostly storm surge) contributions to the total sea level. The residual signal was processed with a high-pass digital filter (with a cut-off period of 10h; Ferrarin *et al.*, 2021) in the spectral domain, with a Fourier decomposition. The decomposition allowed us to isolate the high-frequency sea-level oscillations associated with the mesoscale perturbations, which are assumed to have time scales of $\mathcal{O}$(10 min)–$\mathcal{O}$(1 hr), from the synoptic perturbations. See Ferrarin *et al.* (2021, 2022) for further details on the signal decomposition procedure.

2.2 | Modelling approach

The open-source 3D System of HydrodYnamic Finite Element Modules (SHYFEM; Umgiesser *et al.*, 2014) (https://github.com/SHYFEM-model/shyfem) was applied to simulate the barotropic circulation in the Mediterranean Sea, the Adriatic Sea, and the Lagoon of Venice. With the help of a semi-implicit time-stepping approach and the finite-element method, SHYFEM solves the shallow-water equations. The model has previously been used to examine tidal and nontidal sea-level variations in the Mediterranean Sea (Ferrarin *et al.*, 2013; Ferrarin *et al.*, 2018; Bajo *et al.*, 2019) and for investigating the dynamics of extreme sea storms in the Adriatic Sea, such as the ones occurring in 1966 (Roland *et al.*, 2009), 2018 (Cavaleri *et al.*, 2019), and 2019 (Cavaleri *et al.*, 2020; Ferrarin *et al.*, 2021).

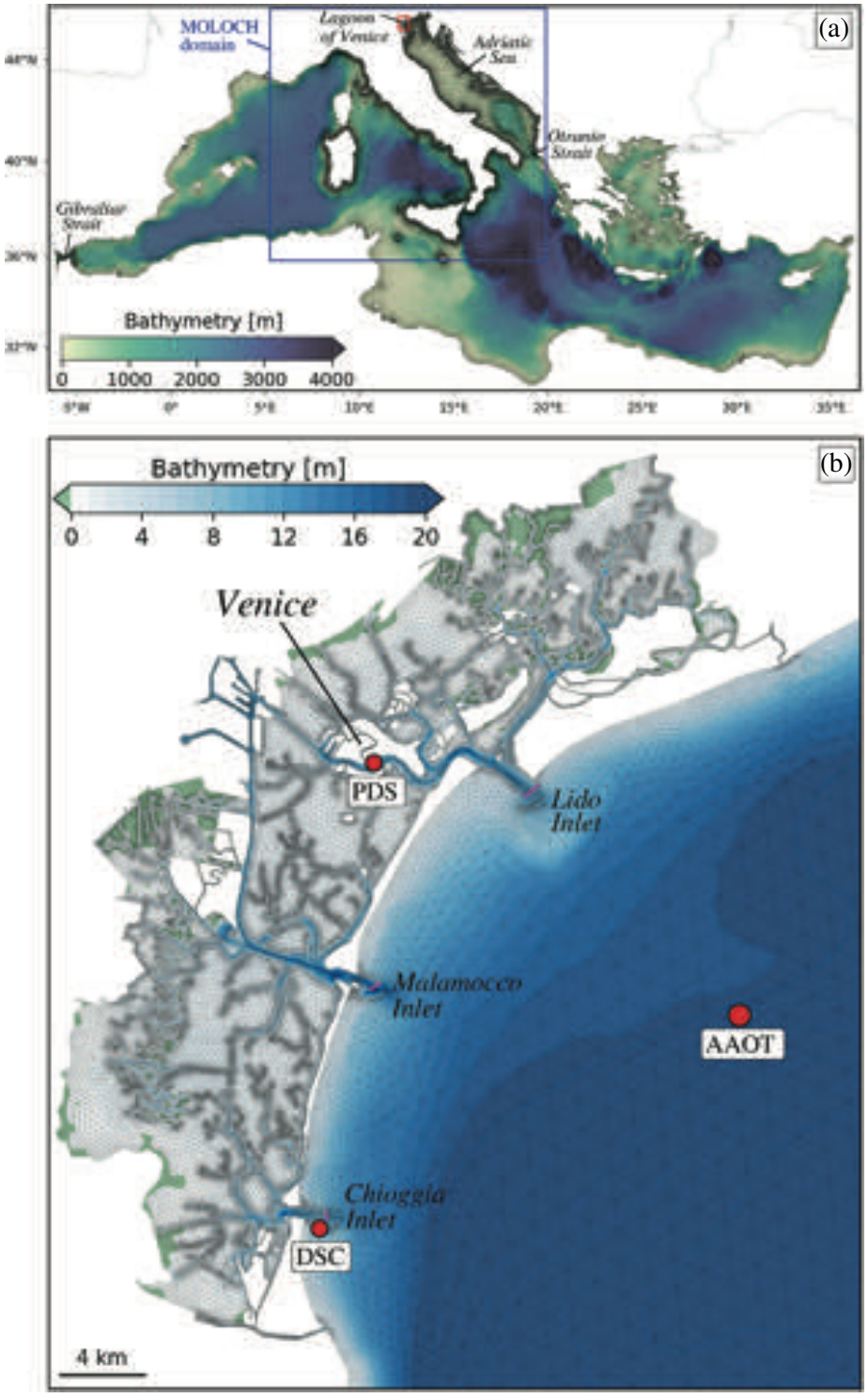

FIGURE 1 (a) Unstructured grid and bathymetry of the Mediterranean Sea, with the blue box indicating the MOLOCH integration domain; (b) zoom of the grid over the Lagoon of Venice with the red dots marking the tide gauges (acronyms are explained in the text). The magenta bars indicate the sea boundaries at the inlets for the simulations that consider only the Lagoon of Venice. [Colour figure can be viewed at wileyonlinelibrary.com]

An unstructured mesh was here used to resolve the phenomenon adequately at various scales, with very high resolution near the coast and in regions of interest. Sea levels during the event were simulated with the SHYFEM model applied on a computational mesh representing the whole Mediterranean Sea and extending into the Atlantic Ocean (up to −6° East). The numerical grid has about 267,000 triangular elements and includes the Po Delta and the northern Adriatic lagoons. The size of the computational elements is variable (Figure 1), with the resolution increasing from the open sea (about 12 km) to coastal waters (2 km) and the narrow channels inside the lagoons (tens of metres).

The Coriolis and pressure gradient terms in the momentum equations and the divergence term in the continuity equation are treated semi-implicitly. The

bottom friction and vertical eddy viscosity are treated completely implicitly for stability reasons, while the remaining terms (advection and horizontal diffusion terms in the momentum equations) are handled explicitly. The free-slip condition is implemented at solid (closed) boundaries. The hydrodynamic model was applied here in its barotropic 2D version with the bottom stress computed using a quadratic bottom drag coefficient set homogeneous over the whole system to a value of 2.5×10^{-3} and the wind stress parametrized following Hersbach (2011) with a Charnock coefficient equal to 0.02. The time step in the simulation was set to 300 s.

The operational model called Iberia–Biscay–Irish (Sotillo *et al.*, 2015) provided detided sea-level (obtained by subtracting the astronomic tide signal from the total sea level) boundary conditions at the Atlantic Ocean boundary. The sea-surface forcing (10-m wind components and mean sea-level air pressure) was provided by the MOLOCH nonhydrostatic, fully compressible, convection-permitting model (Malguzzi *et al.*, 2006; Buzzi *et al.*, 2014). The MOLOCH model is applied over a domain covering Italy and the adjacent seas with an horizontal resolution of 0.0113° (corresponding to 1.25 km) and a vertical discretization consisting of 60 vertical atmospheric levels and 7 soil levels. Wind and mean sea level pressure (MSLP) fields are provided at 15-min intervals. MOLOCH was used to perform a dynamic downscaling of global European Centre for Medium-Range Weather Forecasts (ECMWF) reanalysis (ERA5) fields (Hersbach *et al.*, 2020) over the area of interest. The meteorological forcing over the rest of the hydrodynamic model domain was supplied by the ERA5 reanalysis. For investigating the effect of the local fast-moving cyclone separately, the MSLP and 10-m wind fields were processed with a high-pass filter with a cut-off period of 10 hr. A more detailed description of the signal filtering procedure and the MOLOCH model setup is given in Ferrarin *et al.* (2021).

To analyse the cyclone effect on the sea level, we performed several SHYFEM simulations adopting different configurations and meteorological forcing. The numerical simulations performed are listed here.

1. Validation-ERA5: SHYFEM forced by ERA5 MSLP and wind.
2. Validation-MOLOCH: SHYFEM forced by MOLOCH MSLP and wind.
3. Forcing-hpf: SHYFEM forced by both high-pass filtered MOLOCH MSLP and wind.
4. Forcing-hpf-mslp: SHYFEM forced by only high-pass filtered MOLOCH MSLP.
5. Forcing-hpf-wind: SHYFEM forced by only high-pass filtered MOLOCH wind.
6. Resonance-PG: SHYFEM with a minimum depth of 50 m and forced by high-pass filtered MOLOCH MSLP to examine the possible generation of coastally trapped edge-wave modes (Greenspan resonance). The difference from simulation number 4 is therefore just the modified bathymetry.

To investigate the transformation of high-frequency sea-level perturbations while they enter and propagate in the Lagoon of Venice, the SHYFEM model was applied over a numerical domain representing only the lagoon up to the inlets without the Mediterranean basin and the shelf in front of the lagoon (Figure 1b). In these numerical

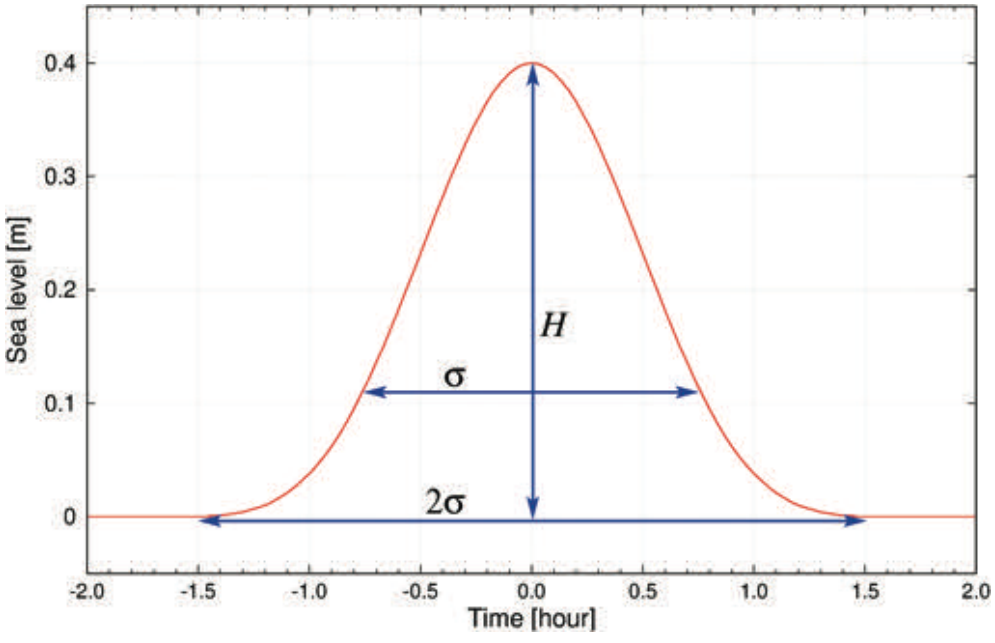

FIGURE 2 Idealized sea-level perturbation as obtained by the Gaspari–Cohn function with amplitude H=0.4 m and width σ=1.5 hr. [Colour figure can be viewed at wileyonlinelibrary.com]

experiments, the model was forced by an idealized sea-level perturbation of amplitude H applied at the inlets and obtained by the Gaspari–Cohn function (Gaspari and Cohn, 1999), which looks like a Gaussian function but values are zero beyond 2σ, where σ is a cut-off distance. We considered several combinations of amplitude (H, ranging from 0.1 to 1 m at intervals of 0.1 m) and width (σ, ranging from 1 to 6 hr at intervals of 20 min) of the perturbation. As an example, Figure 2 shows the water-level perturbation with H=0.4 m and σ=1.5 hr.

3 | RESULTS AND DISCUSSION

3.1 | The November 12, 2019 storm event

The concurrence of several singular processes contributed to the exceptional flood event of November 12, 2019 in Venice: (i) the in-phase timing between the peak of the storm surge and the astronomical tide; (ii) persistent low-pressure and wind systems over the Mediterranean Sea, associated with large-scale low-frequency atmospheric dynamics (planetary atmospheric wave), inducing an anomalously high monthly mean sea level in the Adriatic Sea; (iii) a deep baroclinic low-pressure system over the Tyrrhenian Sea (indicated as L1 in Figure 3a), which generated strong Sirocco (southeasterly) winds along the main axis of the Adriatic Sea, pushing waters to the north; (iv) a fast-moving mesoscale cyclone (with a minimum value of 986.6 hPa recorded at AAOT) embedded in the L1 circulation, travelling in the northwestward direction over the Adriatic Sea along the Italian coast (indicated as L2 in Figure 3a) and generating very strong winds (28 m · s^{-1} on average with 31 m · s^{-1} gusts) over the Lagoon of Venice (Ferrarin *et al.*, 2021). Figure 3b shows that the high-pass filtered meteorological fields isolate the mesoscale cyclone L2 well in the northern Adriatic Sea, characterized by a 4-hPa low-pressure area and winds above 18 m · s^{-1}.

The comparison with the in situ observations presented in Figure 4 shows great improvements in reproducing the cyclone dynamics given by the dynamic downscaling. Indeed, MOLOCH reproduces better the passage of the deep low and related winds in the northern Adriatic Sea with respect to the global ERA5 reanalysis. However, as outlined in Ferrarin *et al.* (2021), the model reproduced the mesoscale cyclone passing above the Po Delta and then moving inland keeping the Lagoon of Venice on its right, while in situ observations suggest that the perturbation travelled along the coast and then moved westward crossing the lagoon. Such a discrepancy in the

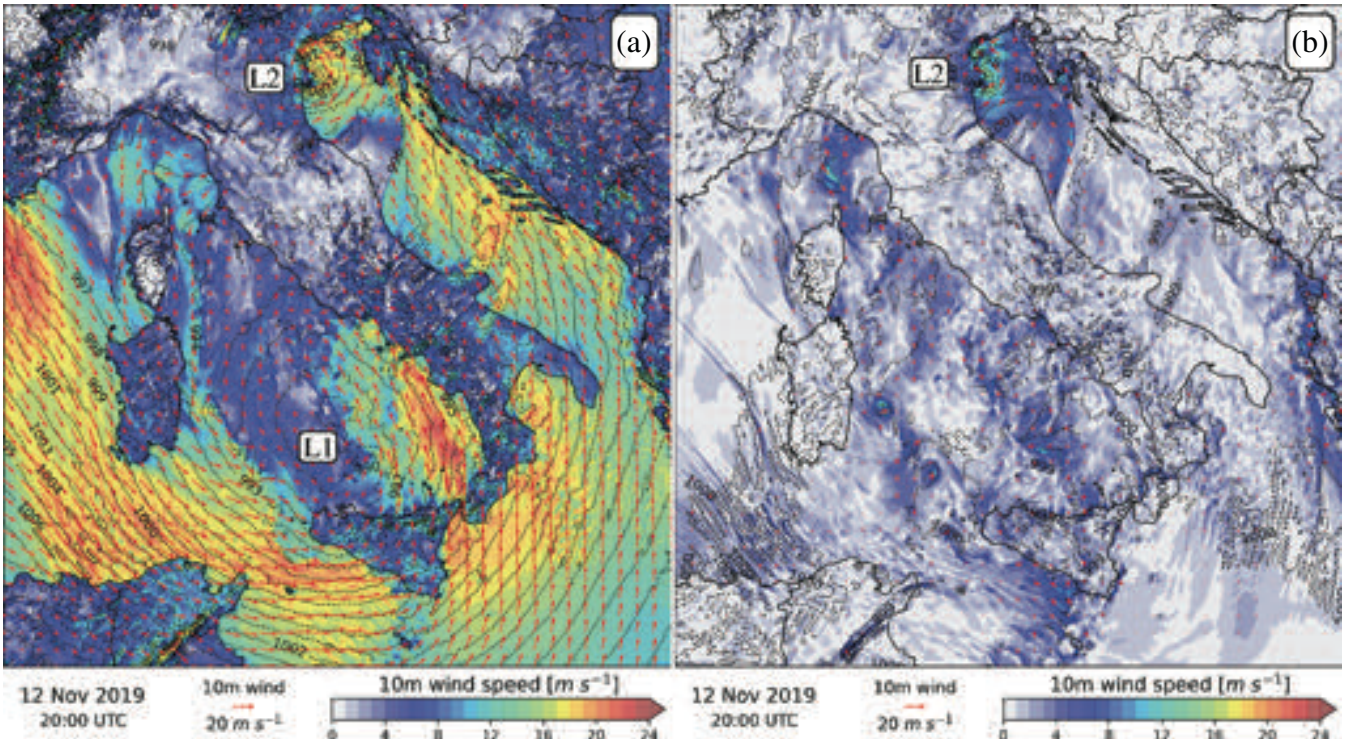

FIGURE 3 (a) Mean sea-level pressure (isolines) and 10-m wind (arrows and colour shading) as simulated by the MOLOCH model on November 12 at 2000 UTC. (b) High-pass filtered (with a cut-off period of 10 hr) MOLOCH fields. Labels L1 and L2 indicate the two low-pressure systems. [Colour figure can be viewed at wileyonlinelibrary.com]

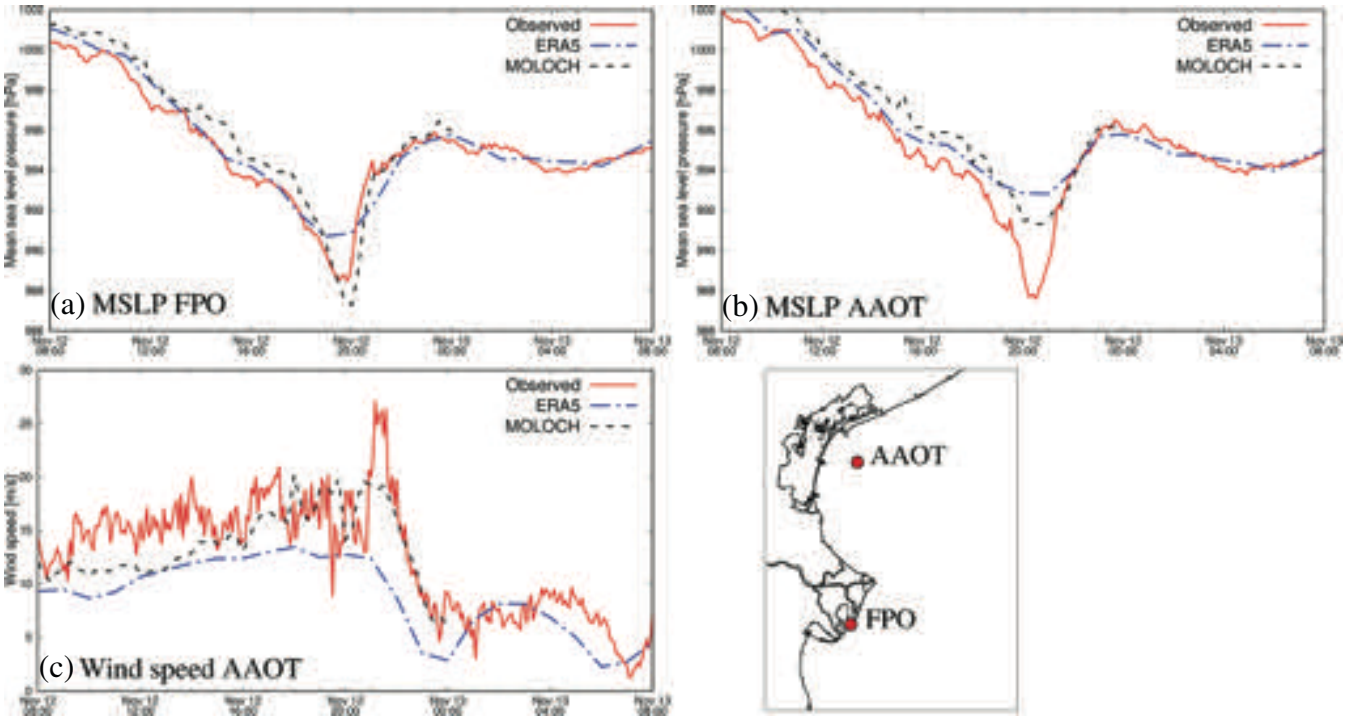

FIGURE 4 Observed and modelled (ERA5 and MOLOCH) mean sea-level pressure and wind speed at AAOT and FPO. [Colour figure can be viewed at wileyonlinelibrary.com]

simulated L2 cyclone track leads to the underestimation of the MOLOCH pressure minimum and wind near the Lagoon of Venice, shown in Figure 4b,c.

As shown in Figure 5, the SHYFEM model forced by the ERA5 reanalysis fields produces a peak residual sea level 1.02 m at in front of the Lagoon of Venice (AAOT). The simulated storm surge is thus more than 0.40 m below the observed peak value. As outlined in Ferrarin *et al.* (2021), this is due to the fact that the low-resolution ERA5 model was not able to reproduce the mesoscale perturbation L2 correctly. In contrast, the hydrodynamic model driven by the high-resolution MOLOCH forcing shows a better representation of the atmospherically driven signal in the open sea. The underestimation of the residual sea level is probably due to the MOLOCH mismatch in the cyclone path.

3.2 | The relative roles of cyclone air pressure and wind forcing

The spectral analysis of the tide-gauge data recorded in front of the Lagoon of Venice (DSC) reveals a high-frequency (period < 10 hr) sea-level perturbation of 35-cm amplitude and 3-hr duration, associated with the passage of the mesoscale cyclone (continuous red line in Figure 6). Different numerical experiments were performed to assess the relative contribution on the peak sea level of the wind and the mean sea-level pressure associated with the mesoscale perturbation. As described in Section 2.2, these simulations (nos 3, 4, and 5) were forced by high-pass filtered meteorological forcing to isolate the effect of the mesoscale cyclone only.

As for other locations (see Figure 5), the model forced by both MSLP and wind shows a sharp rise of sea levels lasting for about 2.5 hr, even if the peak value is underestimated by about 10 cm (Figure 6). Numerical results presented in Figure 6 show that the model forced by the barometric pressure disturbance simulated a storm surge of 12 cm outside the Lagoon of Venice. However, along the Italian coast, the hydrodynamics was also controlled by the shear stress of the winds associated with the mesoscale perturbation, the contribution of which to the simulated sea level is 8 cm. Thus, for this specific mesoscale cyclone, the atmospheric pressure represents the major forcing for the high-frequency sea-level variation in coastal waters.

It is worth noting that the hp-filtered observations could include high-frequency sea-level oscillations driven by forcing and processes not accounted for in the modelling approach, such as nonlinear tide-surge interactions in shallow waters and wind waves. Indeed, the marked drop in the sea level after the peak is not reproduced by the hydrodynamic model. Moreover, the nonlinear transfer of wind energy to the sea via shear stress may also be responsible for the sea-level underestimation when using

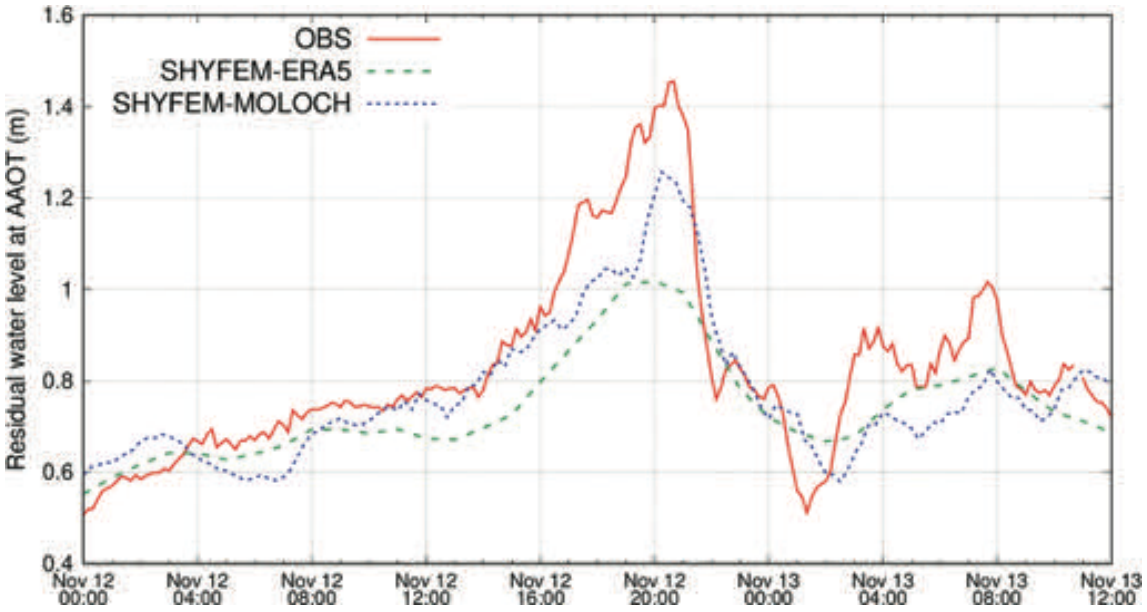

FIGURE 5 Observed and simulated (with both the ERA5 and the MOLOCH forcings) residual (detided) sea levels at AAOT during the November 12, 2019 storm. [Colour figure can be viewed at wileyonlinelibrary.com]

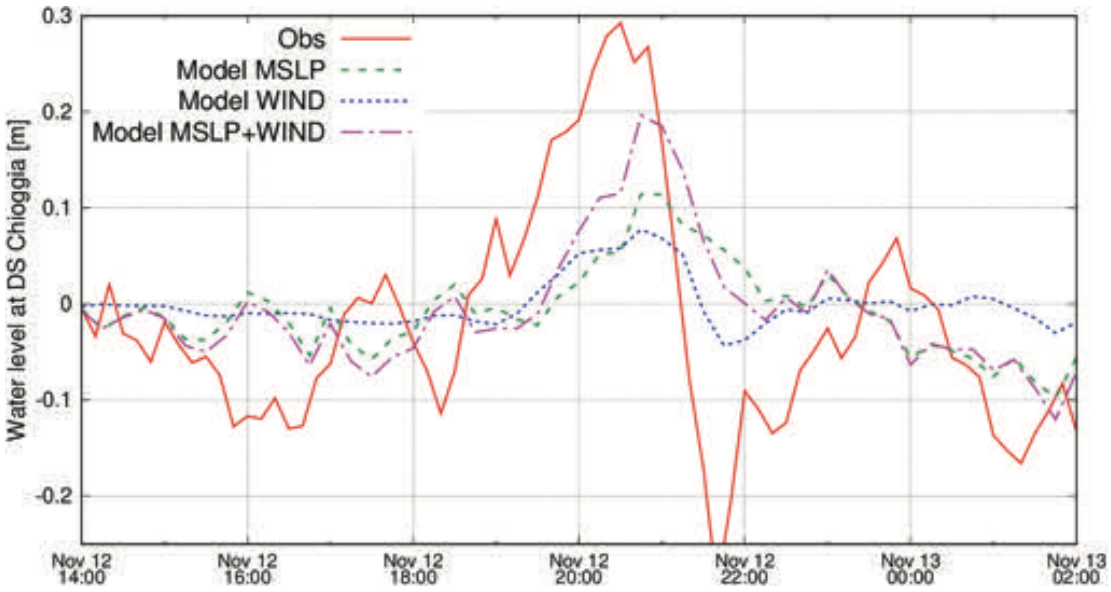

FIGURE 6 Observed and simulated high-frequency (period < 10 hr) sea levels at DS Chioggia. Simulations have been carried out considering hp-filtered MSLP, wind, and MSLP+wind fields. [Colour figure can be viewed at wileyonlinelibrary.com]

filtered forcing (i.e., the sum of the sea levels obtained by forcing the model with separate wind elements is not equal to the sea level estimated using the total wind).

3.3 | Occurrence of atmosphere–sea resonance

The predominant role of the atmospheric pressure associated with the mesoscale cyclone at sea levels could be due to the occurrence of resonant coupling with the sea. To dig into the possible resonance processes of moving local atmospheric depression L2, we compare the hydrodynamic results of the simulation forced by the high-pass filtered MSLP fields with the contribution associated with the static response of sea level to the mean sea-level atmospheric pressure variations (the inverse barometer effect—IBE—which considers a sea-level variation of 1 cm for 1-hPa MSLP variation). IBE was computed over the whole Mediterranean domain and for the whole duration of the event considering high-pass filtered MSLP fields.

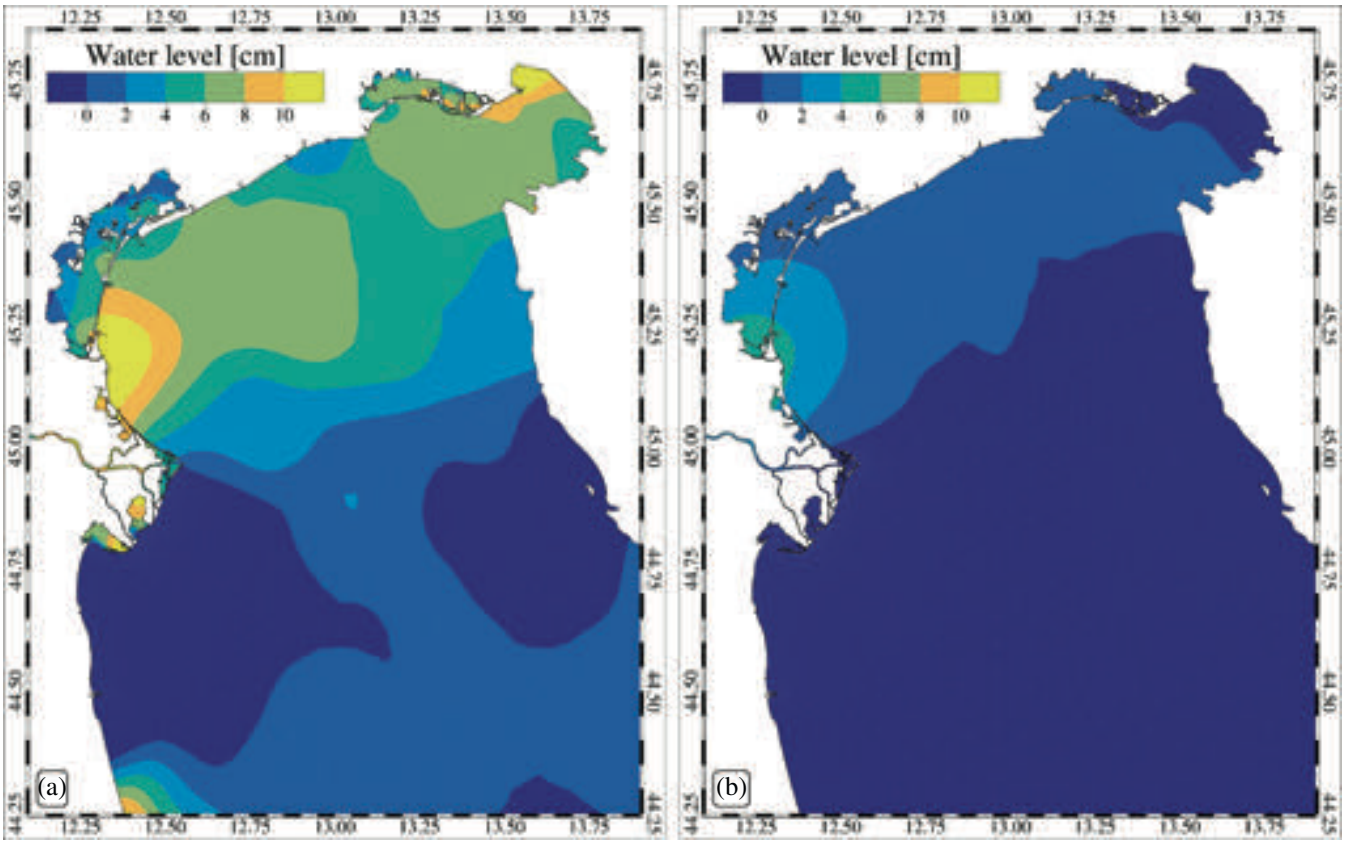

FIGURE 7 (a) Water-level distribution obtained by the SHYFEM model forced by high-pass filtered MSLP and (b) the inverse barometer effect. Both images refer to the situation on November 12, 2019 at 2100 UTC. [Colour figure can be viewed at wileyonlinelibrary.com]

Amplification of the forced wave becomes large near resonance, which happens when the travelling speed of the disturbance approaches the shallow-water wave speed (Proudman, 1929; Pattiaratchi and Wijeratne, 2015). In the 2019 event, the mesoscale cyclone propagated at a speed of about 12 m · s^{-1} over Italian coastal waters having depths of $\mathcal{O}$(10 m). Figure 7 shows that the model forced by the barometric pressure disturbance (waters having depths of $\mathcal{O}$(10 m). Figure 7a) produces water levels near the Venetian littoral higher than those obtained by IBE (waters having depths of $\mathcal{O}$(10 m). Figure 7b). Therefore, these numerical results indicate that atmospheric–ocean resonance processes were at work and that the fast-moving depression generated a meteotsunami-like wave (Monserrat *et al.*, 2006) travelling along the Italian coast. Such a meteotsunami propagated along the Italian coast and entered into the coastal lagoons of the Po Delta, raising the sea level up to values above 10 cm. High sea levels are found also in the upper end of the Adriatic Sea (Gulf of Trieste), probably due to local resonance and bay seiches (Ferrarin *et al.*, 2021). IBE alone results in a much smoother spatial distribution of sea level with respect to the numerical simulation.

The simulated peak value of the sea level outside the Lagoon of Venice (Diga Sud Chioggia) is estimated at 12 cm, which is 8 cm higher than the value obtained with IBE forcing only (Figure 8). Such a threefold inverse-barometer overshoot provides an estimation of the contribution of the meteotsunami to the exceptional flood occurring in the northern Adriatic Sea. The numerical simulation (Model MSLP) reported several sea-level oscillations with amplitude of the order of a few cm, associated with the propagation and amplification of perturbations along the coast and in the northern Adriatic lagoons.

3.4 | Proudman versus Greenspan resonance

The meteotsunami described in the previous section may result from different atmospheric–ocean resonance processes (Pattiaratchi and Wijeratne, 2015). Since the moving speed of the atmospheric disturbance is similar to the local shallow-water wave speed, Proudman resonance (Proudman, 1929) may occur on November 12, 2019. However, since the atmospheric disturbance was travelling parallel to the coast over a sloping bottom, the forced wave could be influenced by Greenspan resonance, exciting coastally trapped edge-wave modes (Greenspan, 1956). To check the occurrence of the different processes, we performed an

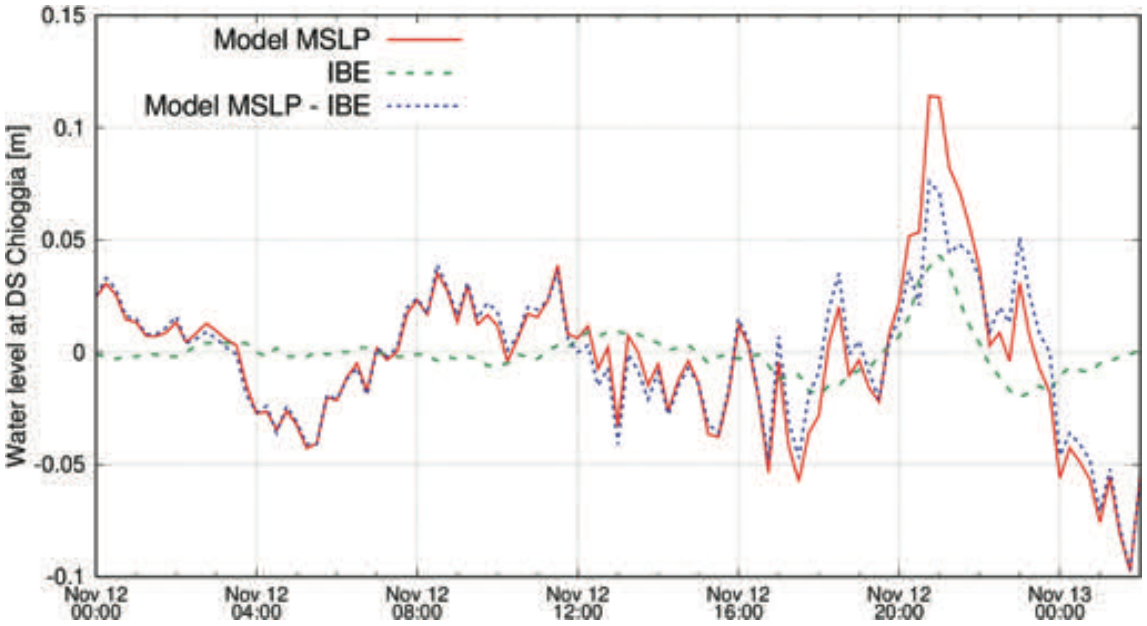

FIGURE 8 High-frequency sea levels at DS Chioggia as simulated by the SHYFEM model forced by the HP-filtered MSLP (continuous red line) and inverse barometer effect (dashed green line). The blue dotted line indicates the difference between model MSLP and IBE. [Colour figure can be viewed at wileyonlinelibrary.com]

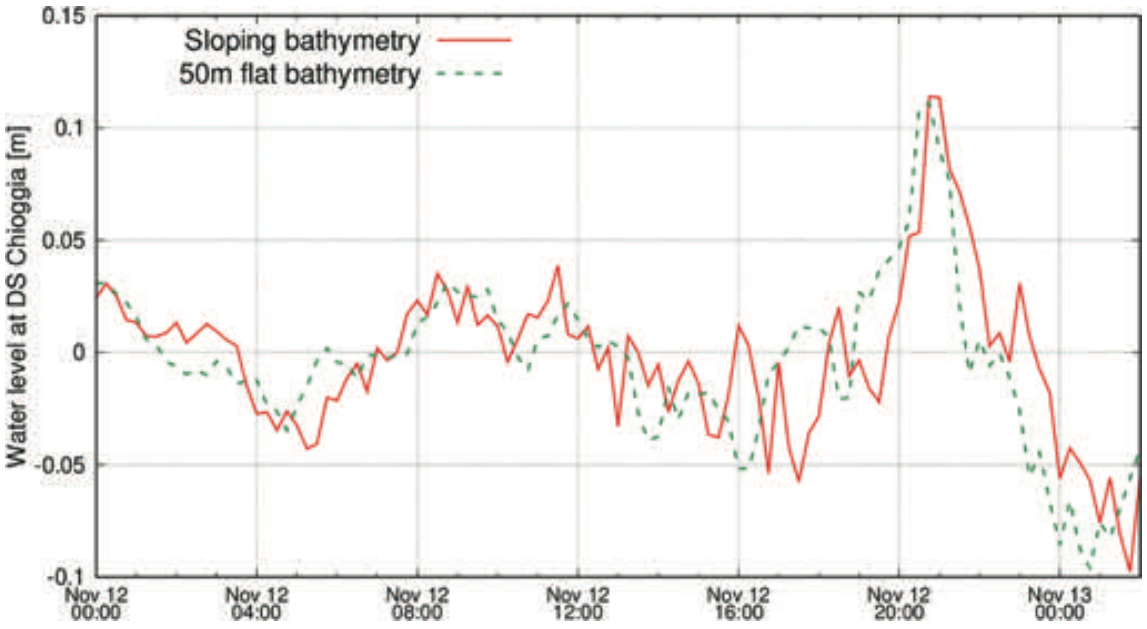

FIGURE 9 High-frequency signal of the water level associated with the L2 cyclone at DS Chioggia as simulated by the SHYFEM model with a sloping bottom (continuous red line) and with a flat bottom of 50 m between the 50-m isobath and the coast in the northern Adriatic Sea (dashed green line). [Colour figure can be viewed at wileyonlinelibrary.com]

additional numerical simulation (named Resonance-PG), using high-filtered MSLP as forcing and setting a fake minimum depth of 50 m over the whole computational grid. Flattering the sea bottom and removing any coastal slopes in the northern Adriatic Sea along the mesoscale perturbation path should exclude the possibility of generating Greenspan resonance.

The results presented in Figure 9 show that the simulated sea levels at the coast have not been influenced significantly by a sloping bottom. These results thus demonstrate that the meteotsunami is initiated mainly through Proudman resonance, since the local weather system is able to transfer energy efficiently into the sea even over a basin with constant water depth. Moreover,

the fact that the results of the two simulations are very similar proves that wave shoaling has not influenced the propagation of the meteotsunami along the coast significantly.

The simulated resonance is in accordance with a simple solution obtained for an idealized flat-bottom rectangular basin having a closed end (Orlić, 1980). For such a case, the author demonstrated that the amplification factor describing the overshoot of the sea-level response with respect to the inverse barometer response via Proudman resonance can be computed as $A = 1/(1 - U/(gH)^{1/2})$, with g the acceleration due to gravity (9.81 m · s^{-2}), H the bottom depth, and U the speed of atmospheric depression that propagates towards the closed end of the basin. Adapting the values to our case (H=50 m and U=12.5 m · s^{-1}) led to an amplification factor A that equals 2.3, which is similar to the threefold inverse barometer overshoot simulated by the model.

3.5 | The sea-level perturbation propagating into the lagoon

According to Lionello *et al.* (2021), northern Adriatic sea-level anomalies first propagate into the lagoon through the three inlets, driven by the hydraulic gradient, and then mainly follow the tidal channels. The behaviour of the signal as it propagates inside the lagoon to the Venice city centre exhibits a strong dependence on frequency. While the amplitude of short-period oscillations (≤ 3 hr) is substantially damped and that of long-period oscillations (≥ 24 hr) is not modified, an internal resonance amplifies intermediate periods (Lionello *et al.*, 2021). This effect depends on the area of the lagoon in question, and the morphology of the seabed is so complex that it is difficult a priori to deduce how the signal will look at a specific point. Further, there are considerable differences in the time required by the signal to propagate from the inlets to different areas of the lagoon. In general, the signal arrives first in the areas most directly connected with the inlets, while in other areas it can suffer considerable delays. Usually, the shape of the tidal and storm-surge signals is such that they, after having entered the lagoon, propagate with small damping to the Venice city centre, where water levels are comparable to the ones close to the inlets, with a typical 1-hour delay (Umgiesser *et al.*, 2004; Ferrarin *et al.*, 2015).

However, despite the vast literature available on the lagoon's hydrodynamics, it is still not clear how high-frequency perturbations, such as the one induced by the mesoscale cyclone that occurred on November 12, 2019, propagate into the lagoon. Several theoretical simulations were performed to analyse the behaviour of a sea level signal similar to that of the 2019 meteotsunami, forced at the three inlets with a sea-level perturbation obtained through a Gaspari-Choln function, as described in the methods section.

The different numerical experiments performed in this study consider a wide range of perturbations, thus allowing the evaluation of propagation and transformation of different types of incoming waves to the whole lagoon and especially to the city centre of Venice. Analysing Figure 10 for Punta Salute, we see that the situation is very complex, as a signal does not always remain unchanged in amplitude, but can be attenuated significantly when it is very narrow, close to the time it takes to arrive at the station of interest. There is therefore damping due to the friction

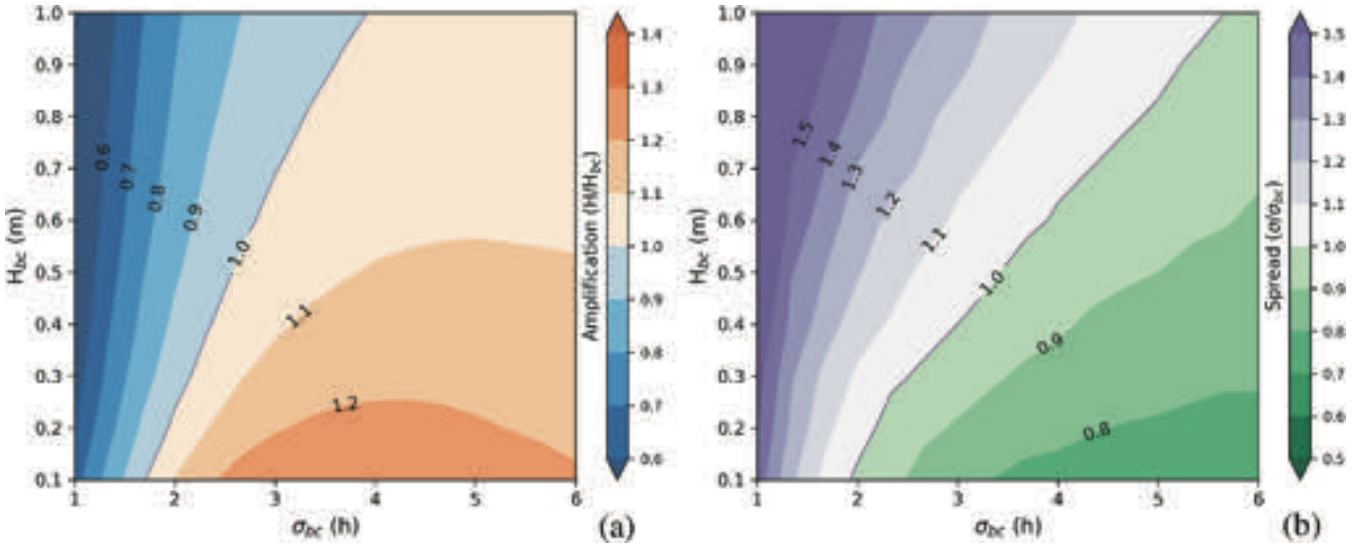

FIGURE 10 (a) Amplification and (b) spread of the sea-level perturbation at Punta della Salute as a function of height (from 0.1–1 m) and width (from 1–6 hr) of the open-boundary forcing. [Colour figure can be viewed at wileyonlinelibrary.com]

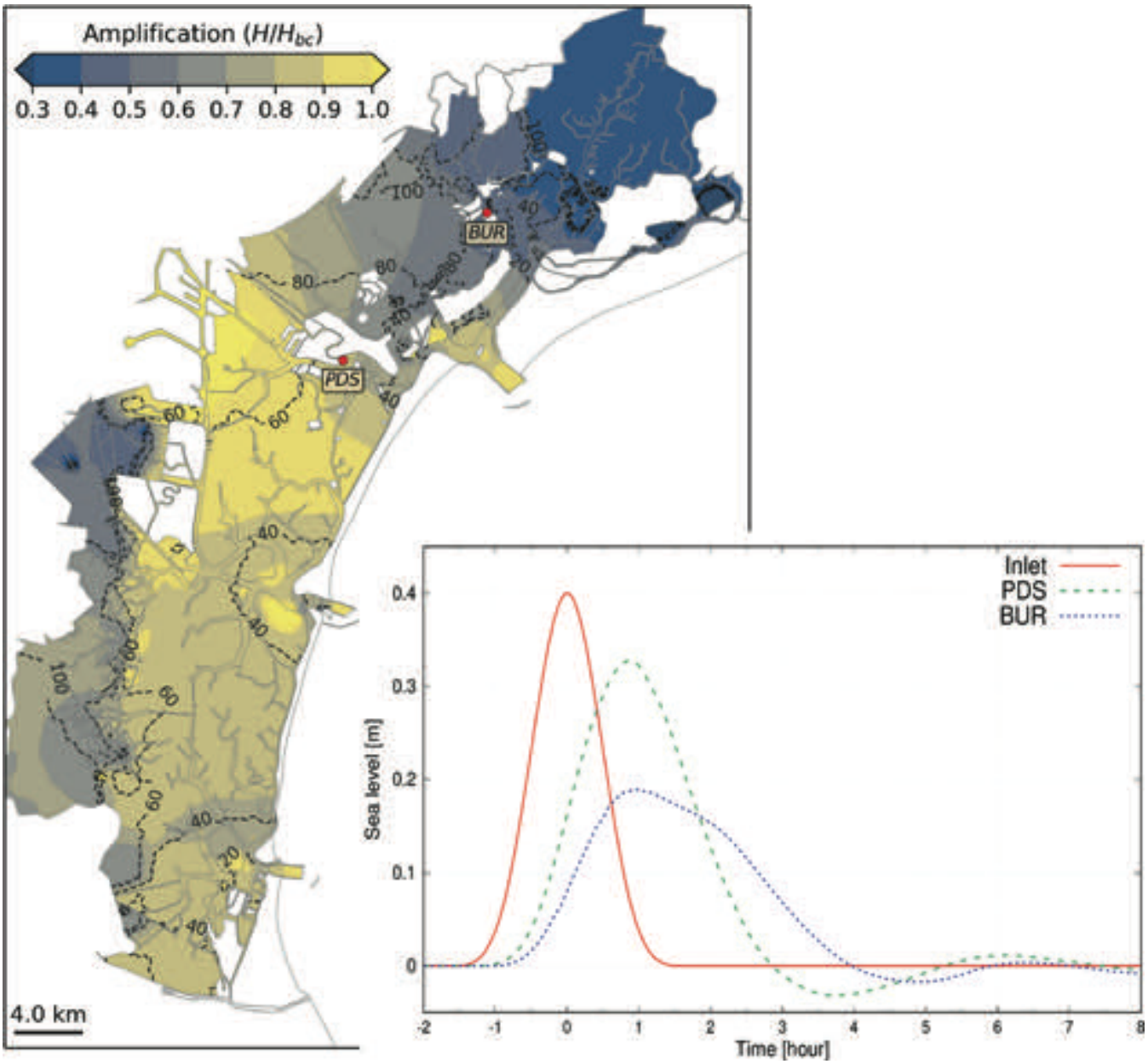

FIGURE 11 Amplification of the perturbation over the Lagoon of Venice as computed by dividing the maximum simulated sea levels by the amplitude of the boundary oscillation (H=0.4 m, σ=1.5 hr). The dashed contour lines report the time delay (in minutes) of the peak of the perturbation. The red dots indicate the location of the analysis points presented in the right panel. [Colour figure can be viewed at wileyonlinelibrary.com]

at the bottom and damping of signals that are short with respect to the time of reaching a specific location.

We found that the time lag between the sea-level peak at Punta della Salute and the inlet forcing does not change significantly as a function of the height and width of the open-boundary forcing. Time-lag values range between 45 and 55 min without a clear pattern.

The transformation of an idealized signal approximating the effect of the meteotsunami inside the lagoon depends strongly on the area, with substantially varying attenuation and broadening. In Figure 11, a signal of amplitude and duration similar to the 2019 event was used. Its propagation inside the lagoon is very different depending on the areas considered. In areas connected to inlets with deep canals and with little friction, such as the southern part of the historic city of Venice, the signal, although delayed by almost an hour, does undergo relatively small damping. In areas further away from the inlets or connected by shallower canals, especially in the northern part of the lagoon, the signal is significantly

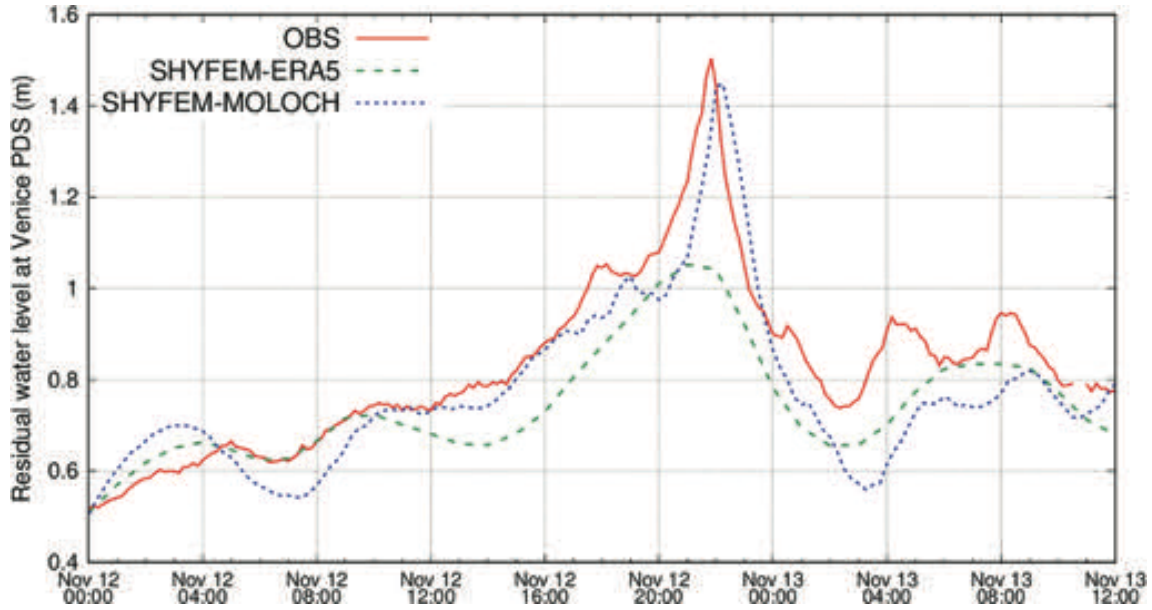

FIGURE 12 Observed and simulated (with both ERA5 and MOLOCH forcings) residual (detided) sea levels at PDS during the November 12, 2019 storm. [Colour figure can be viewed at wileyonlinelibrary.com]

damped, reducing its amplitude to about one-third of the incoming perturbation. The signal peak takes about an hour and a half to reach the remote parts of the lagoon. The central part of the lagoon is where the amplification is greatest. This is because the main channels from the Lido and Malamocco inlets are directed toward this area and the perturbations coming from both inlets overlap.

However, while propagating over the lagoon, the boundary perturbation does not undergo only amplification and damping but also changes shape. The right panel in Figure 11 shows the sea-level time series at the boundary and at Punta della Salute (PDS) and Burano (BUR). In PDS, the sea-level peak is damped by about 20% and the perturbation widens to more than 4 hr. In areas far from the inlets, such as Burano, the signal is strongly damped, loses its Gaussian shape, and widens to about 5 hr.

The capacity of the cross-scale modelling approach in simulating the November 12, 2019 extreme sea level inside the lagoon is demonstrated by the results presented in Figure 12. ERA5 reanalysis does not allow for the generation of the meteotsunami-like wave—driven by small-scale atmospheric disturbance—in the coastal area, and consequently the residual sea level in Venice is strongly underestimated. In contrast, the residual sea levels simulated by the hydrodynamic model forced with MOLOCH data show a good representation of the peak storm signal in Venice, which results from the proper modelling of processes in the open sea (generation and propagation) and the accurate reproduction of transformation of the signal entering the lagoon from the inlets. The sharp peak observed (and simulated) in Venice is also due to the effect of the strong wind over the lagoon in raising the sea level along the city's southern side, estimated at about 10 cm (Ferrarin *et al.*, 2021). Moreover, the strong wind generated steep breaking waves capable of sinking large boats and pontoons and damaging the historic city (Cavaleri *et al.*, 2020).

4 | CONCLUSIONS

The event that occurred on November 12, 2019 is the first documented case of a meteotsunami hitting the Lagoon of Venice. According to Ferrarin *et al.* (2022), this event represents an extremely rare episode. However, full understanding of such a phenomenon deserves specific attention, since it may contribute significantly to coastal flooding and damage.

In this study, we demonstrated that high-resolution numerical models represent valuable tools for investigating the dynamics of such extreme events and evaluating the relative contributions of the different drivers of extreme sea levels. We summarize our main conclusions in the following points.

1. The sea-level extreme registered in Venice was the result of several factors, with the fast-moving mesoscale cyclone contribution being about 40 cm.
2. Mean sea-level pressure was the most significant cause of the sea-level perturbation with respect to the wind, which in any case was not negligible.

3. The fast-moving mesoscale cyclone produced a meteotsunami that travelled in the northwestward direction over the Adriatic Sea along the Italian coast.
4. The meteotsunami was generated by the Proudman resonance, with the travelling speed of the atmospheric disturbance matching the propagation speed of the sea-level signal in the shallow northern Adriatic Sea. Greenspan resonance and wave shoaling have not influenced the propagation of the meteotsunami along the coast significantly.
5. The propagation of a sea-level perturbation inside the lagoon is very complicated, depending on frequency and amplitude. Its magnitude and timing vary substantially depending on the area inside the lagoon, and also amplification caused by internal resonance may occur. However, in the case of the November 12, 2019 meteotsunami, the main effect in the Venice city centre has been small attenuation and broadening of the signal as it propagated from the inlets.

AUTHOR CONTRIBUTIONS

Christian Ferrarin: conceptualization; data curation; formal analysis; funding acquisition; methodology; validation; writing – original draft; writing – review and editing. **Mirko Orlić:** conceptualization; funding acquisition; supervision; writing – original draft; writing – review and editing. **Marco Bajo:** data curation; formal analysis; methodology; software; writing – original draft; writing – review and editing. **Silvio Davolio:** formal analysis; funding acquisition; investigation; methodology; software; writing – original draft; writing – review and editing. **Georg Umgiesser:** methodology; software; supervision; writing – original draft; writing – review and editing. **Piero Lionello:** conceptualization; methodology; supervision; writing – original draft; writing – review and editing.

ACKNOWLEDGEMENTS

This work is part of the COST action CA19109 MedCyclones (European network for Mediterranean cyclones in weather and climate, CA19109) and has been partially supported by the Interreg Italy–Croatia STREAM project (Strategic development of flood management, project ID 10249186). The work done by MO has been supported by the Croatian Science Foundation under project MAUD (IP-2018-01-9849).

CONFLICT OF INTEREST STATEMENT

The authors declare that they have no conflict of interest.

ORCID

Christian Ferrarin https://orcid.org/0000-0003-1172-1463
Marco Bajo https://orcid.org/0000-0002-5969-6386
Silvio Davolio https://orcid.org/0000-0001-8704-1814
Georg Umgiesser https://orcid.org/0000-0001-9697-275X
Piero Lionello https://orcid.org/0000-0002-0779-5681

REFERENCES

Amores, A., Marcos, M., Carrió, D.S. and Gómez-Pujol, L. (2020) Coastal impacts of storm Gloria (January 2020) over the North-Western Mediterranean. *Natural Hazards and Earth System Sciences*, 20, 1955–1968.

Bajo, M., Međugorac, I., Umgiesser, G. and Orlić, M. (2019) Storm surge and seiche modelling in the Adriatic Sea and the impact of data assimilation. *Quarterly Journal of the Royal Meteorological Society*, 145, 2070–2084.

Buzzi, A., Davolio, S., Malguzzi, P., Drofa, O. and Mastrangelo, D. (2014) Heavy rainfall episodes over Liguria in autumn 2011: numerical forecasting experiments. *Natural Hazards and Earth System Sciences*, 14, 1325–1340.

Cavaleri, L., Bajo, M., Barbariol, F., Bastianini, M., Benetazzo, A., Bertotti, L., Chiggiato, J., Davolio, S., Ferrarin, C., Magnusson, L., Papa, A., Pezzutto, P., Pomaro, A. and Umgiesser, G. (2019) The October 29, 2018 storm in northern Italy–an exceptional event and its modeling. *Progress in Oceanography*, 178, 102178.

Cavaleri, L., Bajo, M., Barbariol, F., Bastianini, M., Benetazzo, A., Bertotti, L., Chiggiato, J., Ferrarin, C., Trincardi, F. and Umgiesser, G. (2020) The 2019 flooding of Venice and its implications for future predictions. *Oceanography*, 33, 42–49.

Codiga, D.L. (2011) *Unified Tidal Analysis and Prediction Using the UTide Matlab Functions*. Tech. Rep. 2011-01. Narragansett, RI: Graduate School of Oceanography, University of Rhode Island http://www.po.gso.uri.edu/~codiga/utide/utide.htm.

Ferrarin, C., Bajo, M., Benetazzo, A., Cavaleri, L., Chiggiato, J., Davison, S., Davolio, S., Lionello, P., Orlić, M. and Umgiesser, G. (2021) Local and large-scale controls of the exceptional Venice floods of November 2019. *Progress in Oceanography*, 197, 102628.

Ferrarin, C., Bellafiore, D., Sannino, G., Bajo, M. and Umgiesser, G. (2018) Tidal dynamics in the inter-connected Mediterranean, Marmara, black and Azov seas. *Progress in Oceanography*, 161, 102–115.

Ferrarin, C., Lionello, P., Orlić, M., Raicich, F. and Salvadori, G. (2022) Venice as a paradigm of coastal flooding under multiple compound drivers. *Scientific Reports*, 12, 5754.

Ferrarin, C., Roland, A., Bajo, M., Umgiesser, G., Cucco, A., Davolio, S., Buzzi, A., Malguzzi, P. and Drofa, O. (2013) Tide-surge-wave modelling and forecasting in the Mediterranean Sea with focus on the Italian coast. *Ocean Modelling*, 61, 38–48.

Ferrarin, C., Tomasin, A., Bajo, M., Petrizzo, A. and Umgiesser, G. (2015) Tidal changes in a heavily modified coastal wetland. *Continental Shelf Research*, 101, 22–33.

Ferrarin, C., Valentini, A., Vodopivec, M., Klaric, D., Massaro, G., Bajo, M., De Pascalis, F., Fadini, A., Ghezzo, M., Menegon, S., Bressan, L., Unguendoli, S., Fettich, A., Jerman, J., Ličer, M., Fustar, L., Papa, A. and Carraro, E. (2020) Integrated Sea storm management strategy: the 29 October 2018 event in the Adriatic Sea. *Natural Hazards and Earth System Sciences*, 20, 73–93.

Flaounas, E., Davolio, S., Raveh-Rubin, S., Pantillon, F., Miglietta, M.M., Gaertner, M.A., Hatzaki, M., Homar, V., Khodayar, S., Korres, G., Kotroni, V., Kushta, J., Reale, M. and Ricard, D. (2022)

Mediterranean cyclones: current knowledge and open questions on dynamics, prediction, climatology and impacts. *Weather and Climate Dynamics*, 3, 173–208.

Gaspari, G. and Cohn, S.E. (1999) Construction of correlation functions in two and three dimensions. *Quarterly Journal of the Royal Meteorological Society*, 125, 723–757.

Greenspan, H.P. (1956) The generation of edge waves by moving pressure distributions. *Journal of Fluid Mechanics*, 1, 574–592.

Hersbach, H. (2011) Sea surface roughness and drag coefficient as functions of neutral wind speed. *Journal of Physical Oceanography*, 41, 247–251.

Hersbach, H., Bell, B., Berrisford, P., Hirahara, S., Horànyi, A., Munoz-Sabater, J., Nicolas, J., Peubey, C., Radu, R., Schepers, D., Simmons, A., Soci, C., Abdalla, S., Abellan, X., Balsamo, G., Bechtold, P., Biavati, G., Bidlot, J., Bonavita, M., De Chiara, G., Dahlgren, P., Dee, D., Diamantakis, M., Dragani, R., Flemming, J., Forbes, R., Fuentes, M., Geer, A., Haimberger, L., Healy, S., Hogan, R.J., Hólm, E., Janisková, M., Keeley, S., Laloyaux, P., Lopez, P., Lupu, C., Radnoti, G., de Rosnay, P., Rozum, I., Vamborg, F., Villaume, S. and Thépaut, J.-N. (2020) The era5 global reanalysis. *Quarterly Journal of the Royal Meteorological Society*, 146, 1999–2049.

Lionello, P., Barriopedro, P., Ferrarin, C., Nicholls, R., Orlić, M., Raicich, F., Reale, M., Umgiesser, G., Vousdoukas, M. and Zanchettin, D. (2021) Extreme floods of Venice: characteristics, dynamics, past and future evolution (review article). *Natural Hazards and Earth System Sciences*, 21, 2705–2731.

Lionello, P., Cavaleri, L., Nissen, K., Pino, C., Raicich, F. and Ulbrich, U. (2012) Severe marine storms in the northern Adriatic: characteristics and trends. *Physics and Chemistry of the Earth, Parts A/B/C*, 40-41, 93–105.

Lionello, P., Conte, D. and Reale, M. (2019) The effect of cyclones crossing the Mediterranean region on sea level anomalies on the Mediterranean Sea coast. *Natural Hazards and Earth System Sciences*, 19, 1541–1564.

Malguzzi, P., Grossi, G., Buzzi, A., Ranzi, R. and Buizza, R. (2006) The 1966 "century" flood in Italy: a meteorological and hydrological revisitation. *Journal of Geophysical Research*, 111, D24106.

Marcos, M., Tsimplis, M.N. and Shaw, A.G.P. (2009) Sea level extremes in southern Europe. *Journal of Geophysical Research*, 144, C01007.

Miglietta, M.M. (2019) Mediterranean tropical-like cyclones (Medicanes). *Atmosphere*, 10, 206.

Miglietta, M.M., Buscemi, F., Dafis, S., Papa, A., Tiesi, A., Conte, D., Davolio, S., Flaounas, E., Levizzani, V., and Rotunno, R. (2023). A high-impact meso-beta vortex in the Adriatic Sea. *Quarterly Journal of the Royal Meteorological Society*, 149, 637–656. Portico. https://doi.org/10.1002/qj.4432

Monserrat, S., Vilibić, I. and Rabinovich, A.B. (2006) Meteotsunamis: atmospherically induced destructive ocean waves in the tsunami frequency band. *Natural Hazards and Earth System Sciences*, 6, 1035–1051.

Orlić, M. (1980) About a possible occurrence of the Proudman resonance in the Adriatic. *Thalassia Jugoslavica*, 16, 79–88.

Orlić, M. (2015) The first attempt at cataloguing tsunami-like waves of meteorological origin in Croatian coastal waters. *Acta Adriatica*, 56, 83–96.

Patlakas, P., Stathopoulos, C., Tsalis, C. and Kallos, G. (2021) Wind and wave extremes associated with tropical-like cyclones in the Mediterranean basin. *International Journal of Climatology*, 41, E1623–E1644.

Pattiaratchi, C.B. and Wijeratne, E.M.S. (2015) Are meteotsunamis an underrated hazard? *Philosophical Transactions of the Royal Society A*, 373, 20140377.

Proudman, J.F.R.S. (1929) The effects on the sea of changes in atmospheric pressure. *Geophysical Supplements to the Monthly Notices of the Royal Astronomical Society*, 2, 197–209.

Roland, A., Cucco, A., Ferrarin, C., Hsu, T.-W., Liau, J.-M., Ou, S.-H., Umgiesser, G. and Zanke, U. (2009) On the development and verification of a 2d coupled wave-current model on unstructured meshes. *Journal of Marine Systems*, 78, S244–S254.

Scicchitano, G., Scardino, G., Monaco, C., Piscitelli, A., Milella, M., De Giosa, F. and Mastronuzzi, G. (2021) Comparing impact effects of common storms and Medicanes along the coast of South-Eastern Sicily. *Marine Geology*, 439, 106556.

Sotillo, M.G., Cailleau, S., Lorente, P., Levier, B., Aznar, R., Reffray, G., Amo-Baladron, A., Chanut, J., Benkiran, M. and Alvarez-Fanjul, E. (2015) The MyOcean IBI Ocean forecast and reanalysis systems: operational products and roadmap to the future Copernicus service. *Journal of Operational Oceanography*, 8, 63–79.

Toomey, T., Amores, A., Marcos, M., Orfila, A. and Romero, R. (2022) Coastal hazards of tropical-like cyclones over the Mediterranean Sea. *Journal of Geophysical Research, Oceans*, 127, e2021JC017964.

Umgiesser, G., Ferrarin, C., Cucco, A., De Pascalis, F., Bellafiore, D., Ghezzo, M. and Bajo, M. (2014) Comparative hydrodynamics of 10 Mediterranean lagoons by means of numerical modeling. *Journal of Geophysical Research, Oceans*, 119, 2212–2226.

Umgiesser, G., Melaku Canu, D., Cucco, A. and Solidoro, C. (2004) A finite element model for the Venice lagoon. Development, set up, calibration and validation. *Journal of Marine Systems*, 51, 123–145.

Vilibić, I., Denamiel, C., Zemunik, P. and Monserrat, S. (2021) The Mediterranean and Black Sea meteotsunamis: an overview. *Natural Hazards*, 106, 1223–1267.

Vilibić, I. and Šepić, J. (2009) Destructive meteotsunamis along the eastern Adriatic coast: overview. *Physics and Chemistry of the Earth, Parts A/B/C*, 34, 904–917.

How to cite this article: Ferrarin, C., Orlić, M., Bajo, M., Davolio, S., Umgiesser, G. & Lionello, P. (2023) The contribution of a mesoscale cyclone and associated meteotsunami to the exceptional flood in Venice on November 12, 2019. *Quarterly Journal of the Royal Meteorological Society*, 149(756), 2929–2942. Available from: https://doi.org/10.1002/qj.4539